Journal of ELECTRONIC MATERIALS, Vol. 48, No. 7, 2019
https://doi.org/10.1007/s11664-019-07217-3

Theoretical Analysis of the Cooling Performance of a Thermoelectric Element with Temperature-Dependent Material Properties

CHENGJIAN JU,[1] XUEQIANG WANG,[1] GUANSUO DUI,[1,4] CHRISTOPHER GEORGE UHL,[2] and LIBIAO XIN[3]

1.—Institute of Mechanics, Beijing Jiaotong University, Beijing 100044, China. 2.—Department of Bioengineering, Lehigh University, Bethlehem, PA 18015, USA. 3.—Institute of Applied Mechanics, College of Mechanical and Vehicle Engineering, Taiyuan University of Technology, Taiyuan 030024, China. 4.—e-mail: gsdui@bjtu.edu.cn

Thermoelectric (TE) cooling may play a significant role in the electronic industry in the near future due to advantages such as static cooling and environmentally friendly properties. However, temperature-dependent material properties make theoretical analysis of the cooling performance challenging. In this work, a theoretical model is proposed to predict the performance of a thermoelectric cooler considering the temperature-dependent thermal conductivity, Seebeck coefficient, and electric resistivity. The governing thermal equation of the TE element is given, in which the thermal conductivity and Seebeck coefficient are nonlinear functions of temperature T, while the electric resistivity adopts the value reached at mean temperature. The performance of the TE cooling element, such as temperature field, cooling power, and coefficient of performance (COP), etc., predicted by the proposed model agree well with the numerical and finite element result, which prove the validity of our theoretical model. The results suggest that the temperature-dependent thermal conductivity and Seebeck coefficient have the most notable influence on the heat flow and COP of the TE cooling element.

Key words: Thermoelectric cooling, temperature-dependent, theoretical model, coefficient of performance

INTRODUCTION

In 1823, Thomas J. Seebeck reported that an electromotive force would be produced by a circuit made from two dissimilar conductors when one junction was heated, which is called the Seebeck effect. In 1834, a reverse effect was discovered by Jean Peltier, who observed temperature changes in the junction of a thermoelectric couple between two dissimilar conductors when an electric current was applied, which has come to be called the Peltier effect. Lastly, the Thomson effect relates the rate of heat generation q which results from passing electric current along a portion of a single conductor when a temperature difference ΔT exists in the system. These three effects are called the TE effects.[1–3] The TE cooling devices are based on the Peltier effect which converts electrical energy into a temperature gradient. Figure 1a depicts a TE cooling module considered to be a TE refrigerator. It consists of a number of thermocouples, which typically includes n-type and p-type semiconductors connected electrically in series by metallic connections and thermally in parallel by a top copper connector and two bottom connectors. When a voltage is applied to the thermoelectric cooler (TEC), the electric current is driven from the n-type element to the p-type element.[3] In this process, transport electrons pass from a low energy level inside the p-type element to a high energy

(Received November 3, 2018; accepted April 10, 2019; published online May 7, 2019)

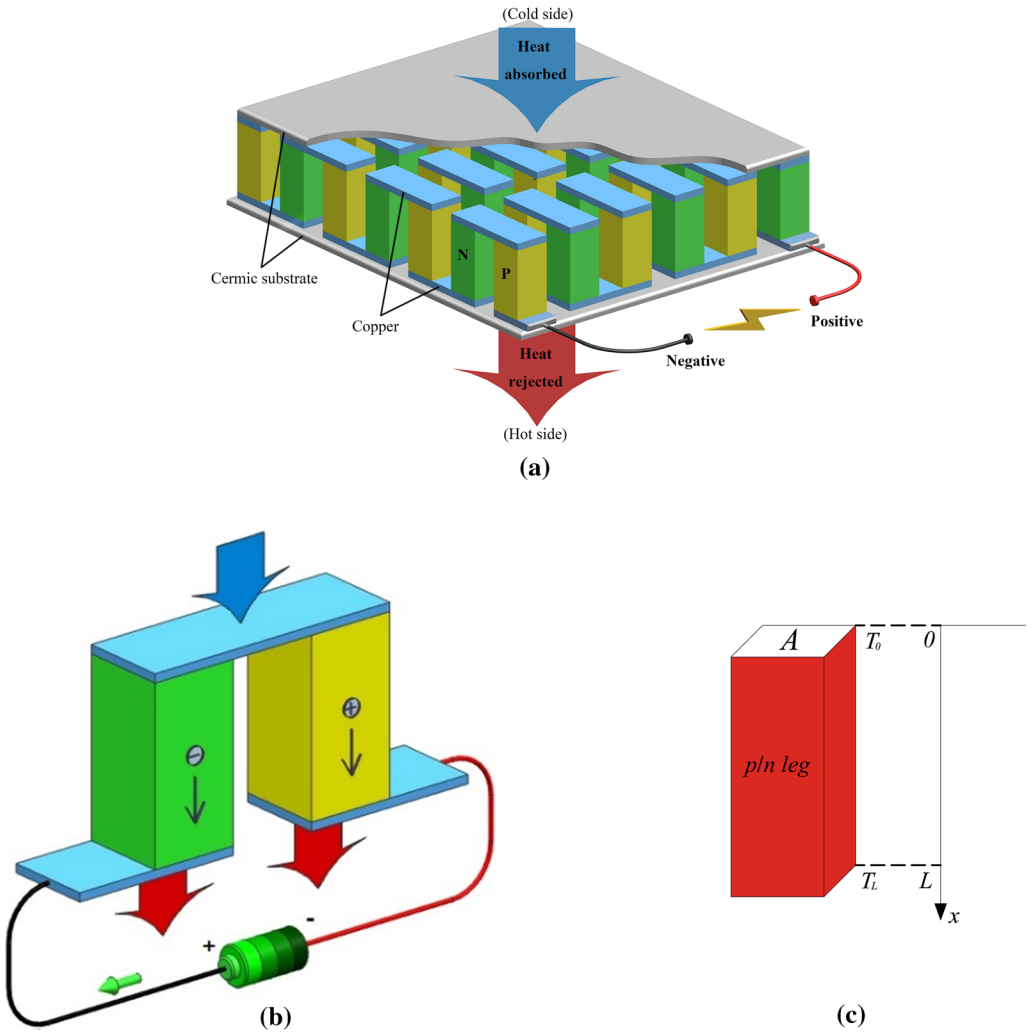

Fig. 1. Schematic illustration of a TEC. (a) a TEC; (b) one of the thermoelectric couples comprising the TEC; (c) a single element (*p* or *n*) with cross section area *A* and length *L*.

level inside the *n*-type element through the cold junction, leading the temperature T_c of the cold junction to decrease. The decrease in the cold junction temperature then facilitates heat transfer from the environment into the cold junction which reduces the temperature of the environment. At the same time, the absorbed heat carried by the transport electrons is transferred to the hot junction, which is at temperature T_h. The heat in the hot junction is then dissipated by a heat sink. Lastly, the electrons return to a lower energy level in the *p*-type TE element and the cycle can begin again. When the electric current is reversed through the system, the hot and cold ends are also reversed.[4,5] The model described above is the theoretical basis used to manufacture TECs or TE pumps.

Compared to traditional refrigeration equipment, the TEC has the advantages of direct energy conversion, compact size and light weight. At the same time, the absence of moving components and refrigerants results in high reliability and low maintenance fees, leading to an increase of the system's lifespan.[6,7] Additionally, a TE microcooler is an ideal candidate for precision temperature control for many opto and electronic devices since they can maintain electronic devices at a desired temperature, such as focal plane arrays in infrared cameras and laser diodes in optical amplifiers.[8] A TEC can also be easily integrated and is a suitable choice for the cooling of such devices because of its static refrigeration features.[9]

To promote the TEC in practical application, it is important to predict the performance of the TEC accurately. A number of researchers have studied the conversion efficiency of TECs in the past two decades. With the assumption of constant material properties, previous works[7,10–13] investigated the performance of TECs. Huang et al.[7] analyzed the influence of the Thomson effect on the performance of a TEC. Seifert et al.[10] built a one-dimension model about TE cooling. Labudovic and Li[11] proposed a three-dimensional finite element analysis of TE cooling. Jeong[12] proposed a new approach to optimize the TE cooling modules. Zhou and Yu[13] presented a theoretical

model for the optimization of a TE cooling system. In their model, the Seebeck coefficient S, electric resistivity ρ and thermal conductivity k were assumed to be constants and the Thomson effect was typically ignored or not properly considered in such cases. However, from some of the experimental results, the TE material properties are actually temperature-dependent.[14–17] The temperature-dependent $Ge_{0.87}Pb_{0.13}Te$ can be seen in Ref. 14. The temperature dependence of material properties for Half-Heusler based semiconducting compounds was also reported in Ref. 15. In addition, Gelbstein and Davidow[16] studied the highly efficient functional $Ge_xPb_{1-x}Te$ based TE alloys. Lalonde[17] reevaluated the n-type $PbTe_{1-x}I_x$, whose material properties are also temperature-dependent. And some researchers suggested that a proper analysis should take the temperature-dependent material properties into account. Hence, it is necessary to take the temperature dependence of material properties into account when studying the performance of a TEC. Moreover, it can be beneficial to give an accurate prediction of the temperature field as it is an important factor to consider for stress analysis.[18] Additional studies[2,7,19] have emphasized the importance of the Thomson effect when dealing with the TE model. The Thomson effect contribution was analyzed using an electrical analogy model in Ref. 2. Chen[19] proposed a numerical model to analyze the performance of miniature TEC affected by the Thomson effect.

In order to take the temperature-dependent material properties into account, some researchers evaluated TE properties using the mean temperature T_m ($T_m = (T_h + T_c)/2$) between the hot (T_h) and cold (T_c) ends.[20,21] Huang[7] has also analyzed the Thomson effect on the performance of the TEC. Yamashita[22] has studied the linear temperature dependence of electric resistivity within a TE system, in which the material properties change linearly with temperature T. Moreover, by assuming the materials properties as nonlinear functions of the temperature, some researchers considered the nonlinear temperature dependence of material properties.[23–28] For example, by using an approximate analytical model, Ju et al.[23] analyzed the performance of the temperature field, energy conversion efficiency and power output for a TE model. Wang et al.,[24] Lv et al.[25] and Gao et al.[26] analyzed the behavior of a two-stage TEC. Through the application of a numerical method, Su et al.[27] investigated the influence of temperature-dependent material properties on the behavior of a TE generator. Also, Kim et al.[28] proposed an engineering dimensionless figure of merit $(ZT)_{eng}$ and an engineering power factor $(PF)_{eng}$, which can predict the practical energy conversion efficiency and power output, respectively. Additionally, Ju et al.[29] studied the influence of temperature-dependent material properties on a functionally graded TE element.

However, most of the models are concentrated on thermoelectric generating cases. For TE cooling, there are not enough theoretical models to predict the performance of TECs accurately. Therefore, it is necessary to build a theoretical model that can predict the performance of TECs with temperature-dependent material properties accurately. In this work, a theoretical model is proposed to predict the cooling performance of TE elements, in which the average electric resistivity is an adopted value, while the Seebeck coefficient and the thermal conductivity used in the proposed model are real values of the system. In this case, the predictions will be more accurate than the model in which all of the materials parameters adopt the set values achieved at the mean temperature. A previous study has proven that temperature-dependent thermal conductivity has a significant influence on the performance of the TE element in some cases.[23] In this work, the proposed model is only applied to the commercially available material Bi_2Te_3, however, the model can also be applied to analyze other types of TE materials[15,30–32] such as the half-Heusler material and lead telluride.

The purpose of this paper is to analyze the cooling performance of a TEC considering the temperature-dependent material properties. In the "Model of a Single TE Element" section, an improved theoretical model is proposed and the approximate analytical solution of the heat equation is obtained. In the "Performance Analysis" section, the performance of a TE element made of the well-known Bismuth Telluride material is analyzed using the proposed model. Concluding remarks are made in the final section.

MODEL OF A SINGLE TE ELEMENT

1D Thermal Energy Balance

As it is displayed in Fig. 1, the basic unit of a TEC is a thermocouple which consists of n-type and p-type semiconductor elements placed electrically in series and thermally in parallel. Figure 1c shows one leg (p or n) of the TE couple and the material properties are a function of temperature T. The TE element studied has a length of L and cross section area A. The temperatures of the cold end and the hot end of the TE element are T_0 and T_L, respectively. The TEC is used to pump heat from the cold side ($x = 0$) to the hot side ($x = L$) through the application of electrical current described by the Peltier effect. The transferred heat is then released to the ambient environment by some external cooling system.

In this paper, to simplify tedious mathematical calculations without altering the heat transfer characteristics and TE effects of the TEC, the following assumptions were made:

1. Heat loss due to heat convection and radiation are neglected, such that the lateral surfaces are considered to be adiabatic[24,25];
2. Dirichlet boundary conditions are used where the temperatures of hot and cold junctions are

constant. Such boundary conditions are used in other works.[33–35] In addition, electric and thermal contact resistances are negligible;
3. One dimensional steady state heat transfer along the axial direction is considered for the analysis.[36]
4. The electric resistivity adopts the mean value.

Based on the above assumptions and the generalized Ohm's and Fourier's laws,[3] the basic equations of thermoelectricity are:

$$j = \frac{E}{\rho} - \frac{S}{\rho}\frac{\mathrm{d}T}{\mathrm{d}x}, \tag{1}$$

$$q = -k\frac{\mathrm{d}T}{\mathrm{d}x} + jST, \tag{2}$$

where j is the electric current density, E is the electric field intensity, ρ is the electrical resistivity, S is the Seebeck coefficient, T is the temperature, q is the heat flux, k is the thermal conductivity, and x is the Cartesian coordinate, respectively. The conservation of energy and continuity of electric current density are expressed as:

$$\frac{\mathrm{d}q}{\mathrm{d}x} = jE, \tag{3}$$

$$\frac{dj}{dx} = 0. \tag{4}$$

From Eq. 1, the following equation can be obtained:

$$E = j\rho + S\frac{\mathrm{d}T}{\mathrm{d}x}. \tag{5}$$

In this work, the effective material properties are adopted, which means the material properties are dependent on temperature T, that is, $S = S(T)$, $\rho = \rho(T)$, and $k = k(T)$. Substituting Eqs. 2 and 5 into Eq. 3, allows Eq. 3 to be reduced to:

$$\frac{\mathrm{d}}{\mathrm{d}x}\left[k(T)\frac{\mathrm{d}T}{\mathrm{d}x}\right] - \frac{I}{A}\mu(T)\frac{\mathrm{d}T}{\mathrm{d}x} + \frac{I^2\bar{\rho}}{A^2} = 0, \tag{6}$$

where $\bar{\rho} = \int_{T_0}^{T_L}\rho(T)\mathrm{d}T \Big/ (T_L - T_0)$, I is the electric current, A is the cross section area of the TE element, and μ is the Thomson coefficient, respectively. According to the second Thomson relationship $\mu = T\mathrm{d}S/\mathrm{d}T$,[3] where S is the Seebeck coefficient.

$S = S(T)$, $\rho = \rho(T)$, and $k = k(T)$ are expressed as quadratic functions of temperature, as in previous studies,[23,24]

$$\begin{aligned} S(T) &= S_0 + S_1T + S_2T^2 \\ \rho(T) &= \rho_0 + \rho_1T + \rho_2T^2 \\ k(T) &= k_0 + k_1T + k_2T^2 \end{aligned} \tag{7}$$

where k_0, k_1, k_2, S_0, S_1, S_2, ρ_0, ρ_1, and ρ_2 are material constants.

With Eq. 7, the second Thomson relationship $\mu = T\mathrm{d}S/\mathrm{d}T$ becomes:

$$\mu(T) = T\frac{\mathrm{d}S}{\mathrm{d}T} = S_1T + 2S_2T^2. \tag{8}$$

And the boundary conditions are:

$$T|_{x=0} - T_0 = 0, \; T|_{x=L} - T_L = 0. \tag{9}$$

Equation 6 can be rewritten in the following form:

$$\frac{\mathrm{d}}{\mathrm{d}x}\left[k(T)\frac{\mathrm{d}T}{\mathrm{d}x}\right] - \frac{I}{A}\bar{\mu}k(T)\frac{\mathrm{d}T}{\mathrm{d}x} - \frac{I}{A}[\mu(T) - \bar{\mu}k(T)]\frac{\mathrm{d}T}{\mathrm{d}x} + \frac{I^2}{A^2}\bar{\rho} = 0, \tag{10}$$

where:

$$\int_{T_0}^{T_L}[\mu(T) - \bar{\mu}k(T)]\,\mathrm{d}T = 0. \tag{11}$$

With the material properties defined in Eqs. 7 and 8, in conjunction with Eq. 11, $\bar{\mu}$ can be obtained as:

$$\bar{\mu} = \left[\left(\frac{1}{2}S_1T_L^2 + \frac{2}{3}S_2T_L^3\right) - \left(\frac{1}{2}S_1T_0^2 + \frac{2}{3}S_2T_0^3\right)\right] \Big/ \left[\left(k_0T_L + \frac{k_1}{2}T_L^2 + \frac{k_2}{3}T_L^3\right) - \left(k_0T_0 + \frac{k_1}{2}T_0^2 + \frac{k_2}{3}T_0^3\right)\right]. \tag{12}$$

Integrating Eq. 10 with respect to x once and using Eq. 7, we have:

$$\frac{\mathrm{d}}{\mathrm{d}x}\left(k_0T + \frac{1}{2}k_1T^2 + \frac{1}{3}k_2T^3\right) - \frac{I}{A}\bar{\mu}\left(k_0T + \frac{1}{2}k_1T^2 + \frac{1}{3}k_2T^3\right) + \frac{I^2}{A^2}\bar{\rho}x + C_1 = 0, \tag{13}$$

where C_1 is a constant.

By allowing $Y = k_0T + 1/2k_1T^2 + 1/3k_2T^3$, Eq. 13 then becomes:

$$\frac{\mathrm{d}Y}{\mathrm{d}x} - \frac{I}{A}\bar{\mu}Y = -\frac{I^2}{A^2}\bar{\rho}x - C_1. \tag{14}$$

And the solution of Eq. 14 is:

$$Y = C_2 e^{\frac{I}{A}\bar{\mu}x} + \frac{I\bar{\rho}}{A\bar{\mu}}x + \frac{A}{I\bar{\mu}}C_1 + \frac{\bar{\rho}}{\bar{\mu}^2}, \tag{15}$$

where:

$$\begin{aligned} C_1 = {} & \frac{I\bar{\mu}}{A}\left[\left(\frac{1}{3}k_2T_0^3 + \frac{1}{2}k_1T_0^2 + k_0T_0\right) - \frac{\bar{\rho}}{\bar{\mu}^2}\right] \\ & - \frac{I^2\bar{\rho}L}{(1-e^{I\bar{\mu}L/A})A^2} - \frac{I\bar{\mu}}{(1-e^{I\bar{\mu}L/A})A} \\ & \times \left[\left(\frac{1}{3}k_2T_0^3 + \frac{1}{2}k_1T_0^2 + k_0T_0\right)\right. \\ & \left. -\left(\frac{1}{3}k_2T_L^3 + \frac{1}{2}k_1T_L^2 + k_0T_L\right)\right] \\ C_2 = {} & \frac{1}{(1-e^{I\bar{\mu}L/A})}\left[\left(\frac{1}{3}k_2T_0^3 + \frac{1}{2}k_1T_0^2 + k_0T_0\right)\right. \\ & \left. -\left(\frac{1}{3}k_2T_L^3 + \frac{1}{2}k_1T_L^2 + k_0T_L\right) + \frac{I\bar{\rho}L}{A\bar{\mu}}\right]. \end{aligned} \tag{16}$$

The temperature profile can be obtained by substituting the acquired C_1 and C_2 into Eq. 15. Since the temperature profile is real and there are three roots of Eq. 15, the two imaginary roots are ignored. The temperature profile is then given as:

$$T(x) = \frac{1}{4k_2}\left[4(\gamma/2)^{1/3} - (2/\gamma)^{1/3}(4k_0k_2 - k_1^2) - 2k_1\right], \tag{17}$$

where:

$$\begin{aligned} \gamma = {} & \frac{1}{4}\left[(6k_0k_1k_2 - k_1^3 - 12k_2^2\beta)\right. \\ & \left. + \sqrt{(4k_0k_2 - k_1^2)^3 + (6k_0k_1k_2 - k_1^3 - 12k_2^2\beta)^2}\right] \\ \beta = {} & -\left(C_2e^{\frac{I}{A}\bar{\mu}x} + \frac{I\bar{\rho}}{A\bar{\mu}}x + \frac{A}{I\bar{\mu}}C_1 + \frac{\bar{\rho}}{\bar{\mu}^2}\right). \end{aligned} \tag{18}$$

$$Q_0 = -Ak(T_0)\left.\frac{dT}{dx}\right|_{x=0} + IS(T_0)T_0, \tag{20}$$

and the heat output at the hot end is:

$$Q_L = -Ak(T_L)\left.\frac{dT}{dx}\right|_{x=L} + IS(T_L)T_L. \tag{21}$$

The input electric power is the difference between the hot and cold heat flow:

$$P = Q_L - Q_0, \tag{22}$$

and the coefficient of performance (COP) is:

$$\mathrm{COP} = Q_0/P. \tag{23}$$

Integration of Eq. 10 once and substitution of the obtained result: $Ak(T)dT/dx$ into Eqs. 20–23, allows for the heat flow input, heat flow output, power output and energy conversion efficiency to be obtained, respectively, as:

$$Q_0 = I\left[S(T_0)T_0 - \bar{\mu}\left(k_0T_0 + \frac{1}{2}k_1T_0^2 + \frac{1}{3}k_2T_0^3\right)\right] + AC_1, \tag{24}$$

$$Q_L = I\left[S(T_L)T_L - \bar{\mu}\left(k_0T_L + \frac{1}{2}k_1T_L^2 + \frac{1}{3}k_2T_L^3\right)\right] + \frac{I^2}{A}\bar{\rho}L + AC_1, \tag{25}$$

$$\begin{aligned} P = {} & I[S(T_L)T_L - S(T_0)T_0 \\ & + \bar{\mu}\left(k_0T_0 + \frac{1}{2}k_1T_0^2 + \frac{1}{3}k_2T_0^3\right) \\ & - \bar{\mu}\left(k_0T_L + \frac{1}{2}k_1T_L^2 + \frac{1}{3}k_2T_L^3\right)] + \frac{I^2}{A}\bar{\rho}L, \end{aligned} \tag{26}$$

$$\mathrm{COP} = \frac{I\left[S(T_0)T_0 - \bar{\mu}\left(k_0T_0 + \frac{1}{2}k_1T_0^2 + \frac{1}{3}k_2T_0^3\right)\right] + AC_1}{I\left[S(T_L)T_L - S(T_0)T_0 + \bar{\mu}\left(k_0T_0 + \frac{1}{2}k_1T_0^2 + \frac{1}{3}k_2T_0^3\right) - \bar{\mu}\left(k_0T_L + \frac{1}{2}k_1T_L^2 + \frac{1}{3}k_2T_L^3\right)\right] + \frac{I^2}{A}\bar{\rho}L}. \tag{27}$$

Performance of the TE Element

At each end of the TE leg, the heat flow $Q(x)$ is given by[23]:

$$Q(x) = -Ak(T)\frac{dT}{dx} + IS(T)T(x). \tag{19}$$

So the heat input at the cold end is:

PERFORMANCE ANALYSIS

In this section, the performance of the TE cooling element is predicted by the proposed theoretical model, numerical method, the analytical model (case 4) in Ref. 20 and the result of the finite element method. For the numerical model, Eq. 6 is solved by the bvp4c function in the MATLAB software. The working condition for the numerical

Table I. Thermoelectric material property of Bi_2Te_3[20,23]

Thermal conductivity	$k(T) = (62605 - 277.7 \times T + 0.4131 \times T^2) \times 10^{-4}$ (W m^{-1} K^{-1})
Electric resistivity	$\rho(T) = (5112.0 + 163.4 \times T + 0.6279 \times T^2) \times 10^{-10}$ (Ω m)
Seebeck coefficient	$S(T) = (22224.0 + 930.6 \times T - 0.9905 \times T^2) \times 10^{-9}$ (V/K)

Only the data was used from Refs. 20 and 23.

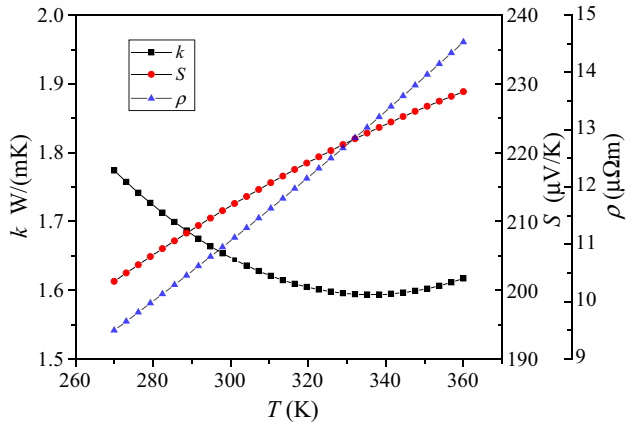

Fig. 2. Material properties of Bismuth Telluride, Bi_2Te_3.[20,23] (only the data was used from these sources) k, S, and ρ represent for thermal conductivity, Seebeck coefficient, and electric resistivity, respectively.

model is the same as the theoretical one, that is, the heat loss from the side surface is neglected. To reduce the computational effort, an analytical model is presented in Ref. 20, in which all the material parameters, like thermal conductivity, electric conductivity, Seebeek coefficients, and Thomson coefficients adopt the values achieved at the mean temperature. The analytical model presented in Ref. 20 is more simple in the mathematical derivation process than the proposed theoretical model, in which only the mean electric resistivity is assumed. A detailed introduction can be found in Ref. 20. The result of the finite element analysis (FEA) is obtained from the commercial software ANSYS. And the heat loss from the side surface is not counted in the FEA simulation. The commercially available Bismuth Telluride Bi_2Te_3 material[20,23] is used in this work and the material parameters are listed in Table I. The length of the TE element is 0.0014 m and the cross-section area is 1.4×10^{-6} m^2. The material properties variation versus temperature are displayed in Fig. 2.

The Temperature Field of the Cooling Element

In this section, the temperature field of the TE cooling element predicted by the proposed model, numerical method, analytical model in Ref. 20 and FEA are displayed in Fig. 3. Figure 3a and b

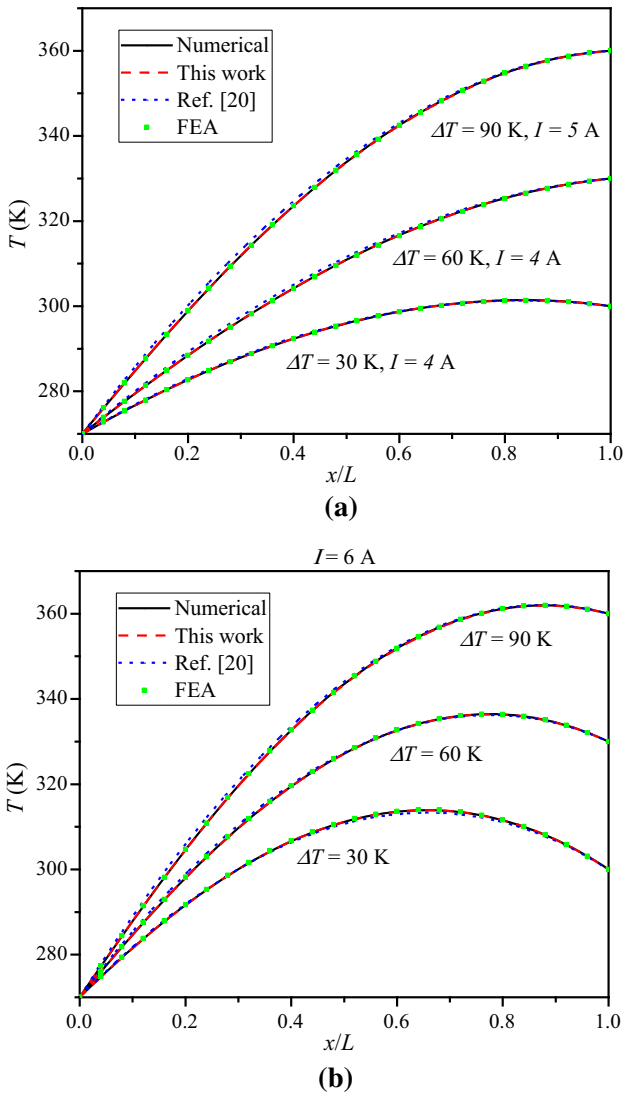

Fig. 3. Variation of temperature versus coordinate x. The electric currents are 4 A, 5 A (a), and 6 A (b), and the working temperature differences are 30 K, 60 K, and 90 K, respectively. The temperature at the cold end (x = 0) is set at 270 K.

correspond to the cases when the electric currents are 4 A, 5 A, and 6 A, respectively, and the working temperature differences of the TE cooling element are 30 K, 60 K, and 90 K. When the working electric current is 4 A, as Fig. 3a shows, the temperature fields predicted by the proposed model agree well with the numerical and FEA results despite the

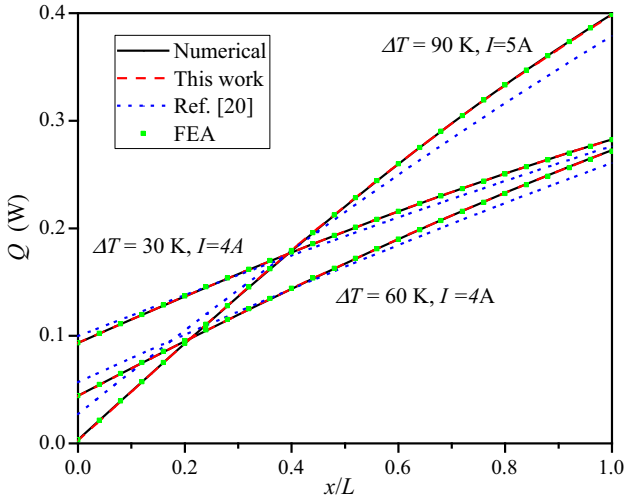

Fig. 4. Variation of heat flow $Q(x)$. The electric currents are 4 A and 5 A. The working temperature differences are 30 K, 60 K, and 90 K, respectively. The temperature at the cold end (x = 0) is set at 270 K.

increase of the temperature difference. The results predicted by the analytical model in Ref. 20 show a little difference from the other models as ΔT increases. When the electric current increases to 6 A, similar trends can be observed in Fig. 3b. In addition, it can be noted that when the electric current is set to 4 A, the temperature increases with the coordinate x. However, when the electric current is set to 6 A, the temperature of the hot end is lower than the middle of the TE element where the highest temperature occurs as shown in Fig. 3b. This occurs because joule heat will play a more important role in the distribution of the temperature field as the electric current increases.

The Heat Flow Distribution of the Cooling Element

In this section, the heat flow variation versus x coordinate is displayed in Fig. 4 for three different working conditions. As is shown in Fig. 4, the heat flow increases as the x coordinate increases from zero to L. When the electric current is 4 A and the temperature difference is 30 K, heat flow increases from about 0.09 W to 0.28 W. At the cold end, the heat flow predicted by the proposed model agrees well with numerical and FEA results. Results predicted by the analytical model in Ref. 20 are a little higher than the proposed model near the cold end, while an opposite trend can be observed near the hot end of the element. When the electric current is 4 A and the working temperature difference is 60 K, the heat flow predicted by the numerical method, the proposed model, and FEA range from about 0.044 W to 0.27 W; while the prediction of the analytical model in Ref. 20 ranges from 0.057 W to 0.26 W. Additionally, for the working condition of 5 A and 90 K, the heat flow variation predicted by the numerical method, the proposed model, and FEA ranges from about 0.003 W to

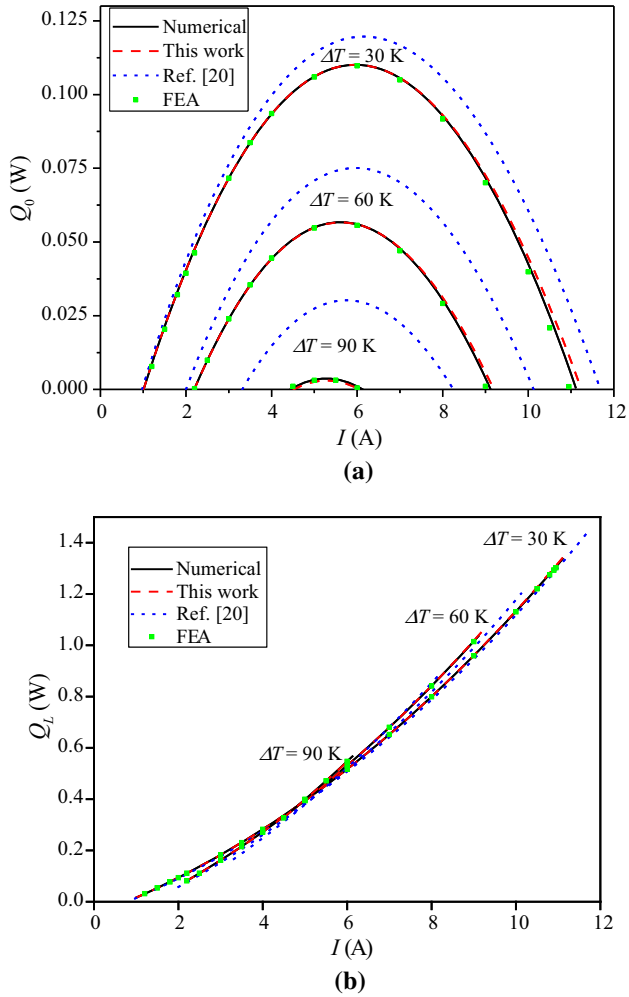

Fig. 5. Variation of cooling power (a) and heat flow output (b) versus electric current. The working temperature differences are 30 K, 60 K, and 90 K, respectively. The temperature at the cold end (x = 0) is set at 270 K.

0.399 W, while the heat flow variation predicted by the analytical model in Ref. 20 ranges from 0.027 W to 0.379 W. It can be observed that the heat input at the cold end decreases as the electric current and working temperature difference increase. Additionally, the heat output at the hot end increases as the electric current and working temperature difference increase.

The Cooling Power (Q_c) and Heat Output (Q_L)

In this section, the cooling power of the TE cooling element predicted by the proposed model, numerical method, finite element method, and analytical model in Ref. 20 are displayed in Fig. 5a, with the working temperature differences being 30 K, 60 K, and 90 K, respectively. It can be seen from Fig. 5a that the cooling power increases as the given temperature difference decreases. When the temperature difference increases to 90 K, the maximum cooling power reduced to nearly zero. Furthermore,

it was observed that the results predicted by the proposed model agree well with numerical and finite element results. The results predicted by the analytical model in Ref. 20 show an evident deviation from the numerical and finite element results, which grow as the temperature increases. When the temperature difference is about 30 K, the deviation is about 8.69% larger than the numerical results, and when the temperature increases to 90 K, the deviation amazingly becomes 900%. This can be attributed to the fact that the material properties are temperature-dependent. The material properties' values at the mean temperature cannot reflect the real case in some conditions, otherwise, improper results will be observed.

Figure 5b plots the heat released from the hot end. The variation trend of the released heat in Fig. 5b is different from Fig. 5a. The heat flow Q_L released from the hot end increases as the electric current increases, and the larger the temperature difference becomes, the less heat is released from the hot end.

Electric Power Input (P)

In this section, the electric power consumed by the thermoelectric element is predicted by the proposed model, numerical method, finite element method, and the analytical model in Ref. 20. As it is clearly shown in Fig. 6, the electric power being used increases as the electric current increases. As the working electric current increases, more joule heat and Thomson heat are produced along the TE element which in turn increases the electric power used to deliver heat. Therefore, the larger the temperature difference becomes, the smaller the effective electric current range is. For the three working conditions tested, the consumed electric power increases as the temperature difference increases when the electric current is the same. It is apparent that results predicted by the proposed model agree well with the numerical and finite element results. When the electric current is held at a small value, the electric power input P predicted by the analytical model in Ref. 20 is somewhat smaller than the predictions by the other three methods for all three of the temperature differences. Additionally, the effective working range of the electric current for the analytical model in Ref. 20 is larger than the other three models. As the temperature difference increases, the differences between the results predicted by the proposed model and the analytical model in Ref. 20 increase, which indicates that the temperature-dependent material properties should be taken into account in the case of relatively large temperature differences.

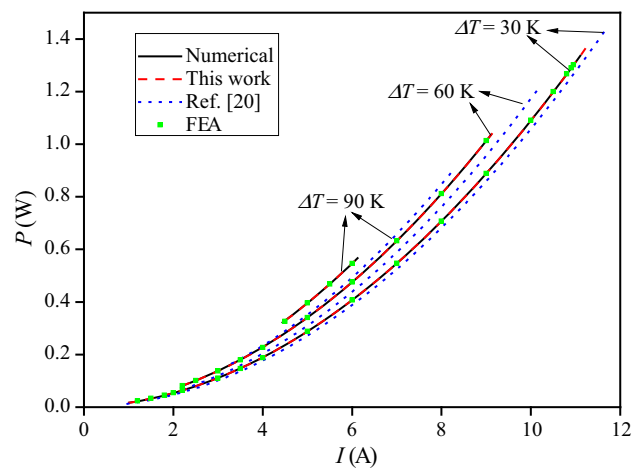

Fig. 6. Variation of electric power input versus electric current. The working temperature differences are 30 K, 60 K, and 90 K, respectively. The temperature at the cold end (x = 0) is set at 270 K.

Coefficient of Performance (COP)

In this section, the coefficient of performance (COP) for the TE cooling element is predicted by the numerical method, the proposed analytical model, finite element method and the analytical model in Ref. 20. Additionally, the simplified model and improved simplified model in Ref. 20 are also presented in Fig. 7 for comparison. A detailed introduction of the simplified model and improved simplified model has been covered in Ref. 20. The realized temperature differences are 30 K, 60 K, and 90 K, and it is assumed that the temperature at the cold end is 270 K. It is evident that the results predicted by the proposed model agree well with the numerical and finite element results. In addition, the predictions of the simplified model and the simplified improved model are almost the same, and the predictions of these two models match the numerical and FEA results well when the electric

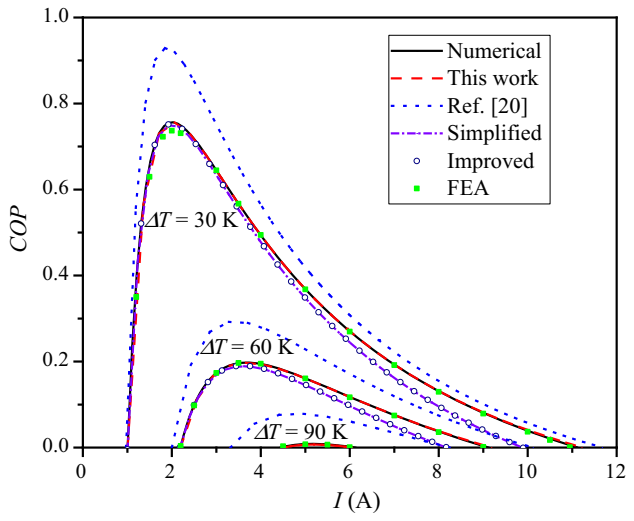

Fig. 7. Variation of coefficient of performance versus electric current. The working temperature differences are 30 K, 60 K, and 90 K, respectively. The temperature at the cold end (x = 0) is set at 270 K. "Simplified" refers to the "Simplified model", and "Improved" refers to the "Improved simplified model". (The details of the "simplified model" and "improved simplified model" are presented in Ref. 20).

currents are smaller than 4A. Under practical working conditions, the working electric current is expected to be near or smaller than the value corresponding to the maximum COP. In this case the simplified and simplified improved model can give a relatively good prediction. However, when the temperature difference is 90 K, the COP predicted by the simplified model and improved simplified model is a negative value, which does not correspond to practical working conditions and, therefore, is not reflected in Fig. 7. This phenomenon may result from neglecting the temperature-dependent thermal conductivity and Seebeck coefficient. Lastly, the prediction of the analytical model in Ref. 20 is much higher than the other three models.

For the three temperature difference conditions, there exist three values of electric current corresponding to the maximum values of the COP. When the temperature difference is 30 K, the electric current corresponding to the maximum COP is about 2 A. For working conditions of 60 K and 90 K, the electric currents corresponding to the maximum COP are around 3.5 A and 4.5 A, respectively. As the temperature difference increases, the relative error between the analytical model in Ref. 20 and the numerical model increases, and the relative deviation at temperature differences of 30 K, 60 K, and 90 K are 22.8%, 48.9%, and 1000%, respectively. This can be attributed to the fact that the thermoelectric material properties are temperature-dependent. Since the temperature field along the TE element is not the same, varied material properties will be exhibited along the length of the TE element. If constant material properties are used to represent the whole TE element, certain errors may result in the performance predictions for the TEC. Additionally, the COP is shown to decrease as the working temperature difference increases. This can be accounted for by the fact that the electric power consumed increases as the temperature difference increases, while the heat absorbed from the cold end decreases as the temperature difference increases.

As is shown in "Coefficient of Performance (COP)" section, the simplified and improved simplified models, which are very simple in their mathematical derivation and clearly covered in Ref. 20, can give a relatively good prediction of the COP for TEC when the electric current is smaller than the value corresponding to the maximum COP. On the other hand, the proposed model, though the mathematical derivation is a little more complex, can take the temperature-dependent thermal conductivity and Seebeck effect into account to produce predictions which agree well with numerical and FEA simulations. Since the simplified and improved simplified model can also give a good prediction of the COP when the electric current and working temperature difference are small, readers can determine which model to use according to the research purpose they want to achieve. As in some cases the simplicity in the process is significant, while the improved accuracy weighs more in some conditions.

CONCLUSIONS

The cooling performance of a thermoelectric element was analyzed by the proposed analytical model, in which the temperature-dependent thermal conductivity and Seebeck coefficient are considered. In the theoretical model, the electric resistivity achieved at the mean temperature was used. The temperature field, heat flow distribution, cooling power, and coefficient of performance predicted by the proposed model agree well with the numerical and finite element results under the same working conditions. If the material properties at the mean temperature are used, the temperature field shows only a small difference from the numerical model and FEA results. However, the predictions of cooling power, electric power input, and coefficient of performance show some deviations from the numerical model and FEA results, especially when the working temperature difference is relatively large. The temperature-dependent thermal conductivity and Seebeck coefficient have notable influence on the heat flow and coefficient of performance. In order to give an accurate prediction of the cooling performance for a thermoelectric model, temperature-dependent material properties should be taken into account when the cooling temperature difference is relatively large. Furthermore, as the working temperature difference increases, the cooling power decreases, while the electric power consumed increases. It is indicated that TECs made of Bismuth Telluride are more suitable to use for cases where the temperature difference is small, since the COP would be relatively large under such conditions. Additionally, the proposed model can be used to predict the mechanical behavior of the TE element since it predicts the temperature field of the TE element accurately, which is closely related to mechanical behavior of the TEC.

ACKNOWLEDGMENTS

This work was supported by National Natural Science Foundation of China (No. 11772041).

REFERENCES

1. H.S. Lee, *Energy* 56, 61 (2013).
2. G. Fraisse, M. Lazard, C. Goupil, and J.Y. Serrat, *Int. J. Heat Mass Transf.* 53, 3503 (2010).
3. D.M. Rowe (ed.), *Thermoelectrics Handbook*: *Macro to Nano*, (New York: Taylor & Francis, 2006), Chapter 1.
4. L.E. Bell, *Science* 321, 1457 (2008).
5. D. Enescu and E.O. Virjoghe, *Renew. Sustain. Energy Rev.* 38, 903 (2014).
6. D. Zhao and G. Tan, *Appl. Therm. Eng.* 66, 15 (2014).
7. M.J. Huang, R.H. Yen, and A.B. Wang, *Int. J. Heat Mass Transf.* 48, 413 (2005).
8. G. Karimi, J.R. Culham, and V. Kazerouni, *Int. J. Refrig.* 34, 2129 (2011).
9. K.H. Lee and O.J. Kim, *Int. J. Heat Mass Transf.* 50, 1982 (2007).

10. W. Seifert, M. Ueltzen, and E. Müller, *Physica Status Solidi (A)* 194, 277 (2002).
11. M. Labudovic and J. Li, *IEEE Trans. Compon. Packag. Technol.* 27, 724 (2004).
12. E.S. Jeong, *Cryogenics* 59, 38 (2014).
13. Y. Zhou and J. Yu, *Int. J. Refrig* 35, 1139 (2012).
14. Y. Gelbstein, J. Davidow, S.N. Girard, D.Y. Chung, and M. Kanatzidis, *Adv. Energy Mater.* 3, 815 (2013).
15. O. Appel, T. Zilber, S. Kalabukhov, and Y. Gelbstein, *J. Mater. Chem. C* 3, 11653 (2015).
16. Y. Gelbstein and J. Davidow, *Phys. Chem. Chem. Phys.* 16, 20120 (2014).
17. A.D. LaLonde, Y. Pei, and G.J. Snyder, *Energy Environ. Sci.* 4, 2090 (2011).
18. S.Y. Yang and G.S. Dui, *Int. J. Solids Struct.* 50, 3254 (2013).
19. W.H. Chen, C.Y. Liao, and C.I. Hung, *Appl. Energy* 89, 464 (2012).
20. G. Fraisse, J. Ramousse, D. Sgorlon, and C. Goupil, *Energy Convers. Manag.* 65, 351 (2013).
21. M. Ibañez-Puy, J. Bermejo-Busto, C. Martín-Gómez, M. Vidaurre-Arbizu, and J.A. Sacristán-Fernández, *Appl. Energy* 200, 303 (2017).
22. O. Yamashita, *Appl. Energy* 85, 1002 (2008).
23. C. Ju, G. Dui, H.H. Zheng, and L. Xin, *Energy* 124, 249 (2017).
24. T.H. Wang, Q.H. Wang, C. Leng, and X.D. Wang, *Appl. Energy* 154, 1 (2015).
25. H. Lv, X.D. Wang, J.H. Meng, T.H. Wang, and W.M. Yan, *Appl. Energy* 175, 285 (2016).
26. Y. Gao, H. Lv, X. Wang, and W. Yan, *Int. J. Heat Mass Transf.* 114, 656 (2017).
27. S. Su, T. Liu, J. Wang, and J. Chen, *Energy* 70, 79 (2014).
28. H.S. Kim, W. Liu, G. Chen, C.-W. Chu, and Z. Ren, *Proc. Natl. Acad. Sci.* 112, 8205 (2015).
29. C. Ju, G. Dui, C.G. Uhl, L. Chu, X. Wang, and Y. Liu, *J. Electron. Mater.* 1, 1 (2019).
30. O. Appel, M. Schwall, D. Mogilyansky, M. Köhne, B. Balke, and Y. Gelbstein, *J. Electron. Mater.* 42, 1340 (2013).
31. Y. Gelbstein, *J. Electron. Mater.* 40, 533 (2011).
32. R. Vizel, T. Bargig, O. Beeri, and Y. Gelbstein, *J. Electron. Mater.* 45, 1296 (2016).
33. T.T. Wallace, Z.H. Jin, and J. Su, *J. Electron. Mater.* 45, 2142 (2016).
34. Z.H. Jin, T.T. Wallace, R.J. Lad, and J. Su, *J. Electron. Mater.* 43, 308 (2014).
35. Z.H. Jin and T.T. Wallace, *J. Electron. Mater.* 44, 1444 (2015).
36. K. Zabrocki, E. Müller, and W. Seifert, *J. Electron. Mater.* 39, 1724 (2010).